

SPECTRAL MEASUREMENTS OF TEMPERATURE AND LONGITUDINAL VELOCITY FLUCTUATIONS IN FULLY DEVELOPED PIPE FLOW

K. BREMHORST and K. J. BULLOCK

Department of Mechanical Engineering, University of Queensland, Brisbane, Australia

(Received 30 May 1969 and in revised form 4 November 1969)

Abstract—It is known that for fully developed flows the similarity between heat and momentum transfer can be studied in terms of the temperature and longitudinal velocity fluctuations at a point. Results of spectral and cross-spectral measurements are presented which show that a strong relationship exists between the velocity and temperature field at low wavenumbers but not at high wavenumbers. Considerable flow energy was found associated with wavelengths much larger than the tube diameter and new information about spectral shapes is revealed. From Taylor's hypothesis and time delayed cross-correlations, the streamwise extent of the correlation between the two fields is described.

NOMENCLATURE

a ,	radius of tube = 2.67 in.;	$R_{u\delta}(k_1)$,	cross-correlation coefficient at wavenumber k_1 .
c_p ,	specific heat at constant pressure [Btu/lb °F];	$R_{u\delta}(x)$,	total spatial cross-correlation coefficient with u and δ separated by distance x ;
C_x ,	convection velocity [ft/s];	t ,	local static temperature [°F];
e ,	voltage;	t_{\min} ,	minimum static temperature at a given value of x [°F];
$E(k_1)$,	fraction of energy of $\overline{u^2}$ associated with $k_1 = \frac{\overline{u^2}(k_1)}{\overline{u^2}}$;	t_w ,	wall temperature [°F];
f ,	friction factor;	T_v ,	friction temperature = $\frac{q_w''}{\rho c_p U_t}$ [°F];
$G(k_1)$,	fraction of energy of $\overline{u\delta}$ associated with $k_1 = \frac{\overline{u(k_1)\delta(k_1)}}{\overline{u\delta}}$;	u ,	longitudinal velocity fluctuation [ft/s];
k_1 ,	one-dimensional wavenumber [ft ⁻¹] = ω/C_x ;	$u(k_1)$,	longitudinal velocity fluctuation at wavenumber k_1 [ft ² /s] ¹ ;
K ,	constant;	$\overline{u(k_1)\delta(k_1)}$,	cross-spectral density of $\overline{u\delta}$ [ft °F/s];
n ,	cyclic frequency [s ⁻¹];	U ,	local mean velocity [ft/s];
q_w'' ,	heat flux at wall [Btu/h °F ft ²];	U_τ ,	friction velocity [ft/s];
Re ,	Reynolds number based on bulk velocity and tube diameter;	\overline{U} ,	bulk velocity [ft/s];
Re_{0a} ,	Reynolds number based on velocity at centre line and radius of tube;	x ,	stream-wise distance [ft];
$R_{u\delta}$,	total cross-correlation coefficient;	y ,	radial distance from wall [in.];

y^+ ,	non-dimensional distance from wall = yU_w/ν .	boundary layer flow. However, since Johnson measured only total correlations, their wavenumber dependence remained unknown.
Subscripts		
A ,	amplifier;	Fluctuating components may be thought of as fluid lumps of varying size meandering throughout the flow region relatively randomly, or as definite flow patterns in the form of organised eddies, or as wavelike behaviour which is suggested by experimental evidence for some regions of the flow. For the present purposes it is unimportant which of these models is preferred. The only assumption used is that the flow field under investigation is stationary in time and can be described in terms of spectral or wavenumber components.
u ,	velocity;	
x ,	X-wire array;	
δ ,	temperature;	
1,	single wire (temperature wire);	
0,	condition at centre line.	
Greek letters		
δ ,	stream temperature fluctuation [$^{\circ}\text{F}$];	Considerable theoretical work has already been done on the prediction in the universal sub-range of the shape of the spectrum of the temperature fluctuations. Thus, Corrsin [4], Obuckhoff [5], Batchelor [6] and Batchelor <i>et al.</i> [7] have predicted that the spectrum has a slope of $-5/3$ in the inertial subrange, -1 for the viscous-convective range for large Prandtl number fluids and $-17/3$ for low Prandtl number fluids. It has also been predicted that in the inertial subrange, the slopes of velocity and temperature spectra are the same.
$\delta(k_1)$,	stream temperature fluctuation at wavenumber k_1 [$\text{ft } ^{\circ}\text{F}$];	
ΔT ,	$t_w - t$ [$^{\circ}\text{F}$];	
$\Gamma(k_1)$,	fraction of energy of $\overline{\delta^2}$ associated with $k_1 = \frac{\overline{\delta^2}(k_1)}{\overline{\delta^2}}$;	
ϵ ,	relative error;	
λ_1 ,	one-dimensional wavelength or wavelength in streamwise direction [ft or in.] = $2\pi/k_1$;	
ν ,	kinematic viscosity [ft^2/s];	
π ,	3.1416;	
ρ ,	mass density [lb/ft^3];	
ω ,	radian frequency [s^{-1}].	
Others		
$ $,	denotes absolute value;	Although these latter considerations apply only to the wavenumber components of total turbulent kinetic energy and the three-dimensional spectrum of the temperature fluctuation, Hinze [9] has argued that for velocity fluctuations this dependence can be expected to be retained for the one-dimensional spectrum. For temperature fluctuations Gibson and Schwarz [8] have shown that the one-dimensional spectrum should also retain this dependence.
\sim ,	denotes approximate response.	

INTRODUCTION

REYNOLDS analogy (Eckert and Drake [1]) or the reduction of the Navier-Stokes and energy equations (Kestin and Richardson [2]) shows that for a detailed study of turbulent heat transfer the relationship of prime interest is that between the longitudinal velocity fluctuations, u , and the temperature fluctuations, δ . That these two components do, in fact, play a major role in bounded turbulent heat transfer has already been shown by Johnson [3] who found them to be very highly correlated in the wall regions of

For lower wavenumbers no theoretical work of any kind appears to be available for scalar fields, presumably because of the intractable nature of the problem. The only remaining theoretical guide appears to be for the lower wavenumber regions of the turbulent kinetic energy for which Hinze [10] has shown from Tchen's work that a -1 dependence on wavenumber can be expected.

Experimental work verifying the high wavenumber predictions of the above workers is available in Corrsin [11] behind a heated grid, Gibson and Schwarz [8] for a homogeneous field behind a grid, and most recently by Grant *et al.* [12] for velocity and temperature fluctuations in the open sea and a tidal channel. The feature of all these fields is that no significant scale effect due to the size of the equipment existed.

For fully developed pipe flow the work of Tanimoto and Hanratty [13] and Rust and Sesonske [14] does not show any of the spectral trends mentioned above although the latter authors thought that this may have been due to the lack of spatial resolution because of the relatively large probe used as their sensing element.

The quantity which has received least attention so far is the cross-correlation between the temperature and velocity fluctuations. Johnson [3] has reported some such measurements for bounded flow and Corrsin and Uberoi [15] for a heated jet. However, no measurements of cross-spectral correlations are available.

At high wavenumbers, well above those representing the energy-containing eddies, the velocity and temperature field become independent of their formation and the correlation between u and δ at these wavenumbers should be negligible. In the energy-containing range and at lower wavenumbers, the opposite can be expected but the exact distribution of the correlation would depend on the flow structure which is still unknown. Therefore, in order to help in the formulation of a mathematical model simulating turbulent heat transfer, measurements of the correlation should be made.

As the measurement of three-dimensional spectra is a task of considerable magnitude, only one-dimensional spectra were measured at this stage.

METHODS OF PRESENTATION OF SPECTRAL DATA

Two methods are adopted. Firstly, a linear-log plot with the ordinate $k_1 \cdot E(k_1)$ and abscissa

proportional to $\ln k_1$; and secondly, the conventional log-log plot of $\ln E(k_1)$ and $\ln k_1$. The first method, which is rarely used, is very sensitive to changes in the energy distribution and is in sharp contrast to the second method. In addition the area under any section of the $k_1 \cdot E(k_1)$ plot represents the fraction of total energy in that wavenumber range. $E(k_1)$ is defined such that

$$\int_0^{\infty} k_1 E(k_1) d \ln k_1 = 1.0. \quad (1)$$

Similarly, $\Gamma(k_1)$ is defined for the fluctuating temperature signal such that

$$\int_0^{\infty} k_1 \Gamma(k_1) d \ln k_1 = 1.0. \quad (2)$$

The cross-spectral function of u and δ i.e. $G(k_1)$, is also defined so that

$$\int_0^{\infty} k_1 G(k_1) d \ln k_1 = 1.0. \quad (3)$$

In order to facilitate comparison of the present results with those already available, those predicted by theory and to assist in the identification of the most energetic flow components, some of the data are also plotted on the conventional log-log plot.

EXPERIMENTAL APPARATUS

The working section of the wind tunnel used for the present results consisted of a horizontally mounted 5.34 in. i.d., 0.375 in. wall thickness, 29 ft 8 in. long extruded aluminium tube through which air was forced by a centrifugal fan. A settling chamber designed to eliminate swirl and large scale turbulence generated by the fan and associated diffuser, separated the latter from the pipe. In order to promote flow development a screen and boundary layer trip were placed at the entrance to the tube. The last 17 ft 2 in. of the tube were heated with 0.125 in. dia heating cable wound around the outside of the tube into grooves machined for the purpose.

Traverses were performed 1 ft 9 in. from the down-stream end of the tube by introducing

probes radially through the tube wall. The traversing station was designed and tested to ensure that the wall temperature distribution had not been affected. The critical dimensions were, therefore, 28 tube diameters of unheated flow and 35 tube diameters of heated flow which, as expected from available literature, was shown to produce fully developed flow at the traversing plane. The heating method used produced uniform heat flux which in turn gave a linear wall temperature gradient. A guard heater and appropriate thermal insulation were also provided to ensure no heat losses to the surroundings. For the low heat inputs of the present experiments a.c. heating was used and the heat input measured with a precision watt-meter.

INSTRUMENTATION

Hot wire anemometers were used as sensors in a three-wire array which consisted of a conventional X-meter and a third wire placed at right angles to the plane of the X-meter. The X wires were operated at the highest temperature which still gave rigid wires (thermal expansion at high wire temperatures can be quite serious). These wires, termed velocity wires, responded predominantly to velocity fluctuations. The third wire, the temperature wire, was operated at a very low wire current and, therefore, responded mainly to temperature fluctuations. This wire was placed 0.012 in. upstream of the geometric centre of the X-meter.

In order to minimise any interference from the temperature wire on the X-meter and also to get the best possible signal to noise ratio at the low wire temperature, a 0.0001 in. dia. \times 0.056 in. tungsten wire with copper plated ends was used. At the velocities reported, the wire Reynolds' number for this wire was less than 1.3 and that of the plated ends less than 10. This was found to give negligible flow interference. Lateral separation between the inclined wires of the X-meter was 0.015 in. The velocity wires were of 0.0004 in. dia. \times 0.055 in. platinum-rhodium-ruthenium alloy (Sigmund-Cohn type 851) which is

extremely stable both dimensionally and electrically.

A single wire could, of course, have been used instead of the X-meter but since the present results were part of a larger project, only X-meter data were collected.

The anemometer units consisted of Flow Corporation Model HWB constant current bridges each followed by a d.c. off-set network and a Preston Model 8300 high gain, low noise wide band, d.c. coupled differential amplifier. The normal open loop compensation for the time constant of each wire was achieved with a combination of EAI 231-R analogue computer amplifiers and Tektronix Type 3A8 operational amplifiers used for low noise, wide bandwidth differentiation.

For signal r.m.s. values or cross-correlation measurements, squaring or multiplication and integration was carried out on the analogue computer, which allowed any desired integration time to be used. The above signal amplification system gave exceptionally good long term stability with minimum signal distortion.

Spectral measurements were obtained by recording signals proportional to u and δ on a Tolana FM tape recorder. Two Bruel and Kjaer Type 2107 constant percentage bandwidth analysers were used for filtering the signals but signal squaring and averaging was again performed on the computer. In order to cover the desired frequency range it was necessary to record the signals at two different speeds—once at 15 i.p.s. and then at $1\frac{7}{8}$ i.p.s. Replay was always at 15 i.p.s. The frequency response of the combined hot-wire amplification and signal processing equipment was flat to within 2 per cent up to 2 KC which was quite adequate. A simple R-C filter with a 2 s time constant was used to remove any d.c. levels prior to signal processing. No error was produced by phase effects provided care was taken to use matched signal channels. Analyser noise bandwidths were 10.5 per cent of the centre frequency.

Since ideal responses to velocity and temperature fluctuations cannot be obtained practically,

a unique signal correction procedure was employed to eliminate the small temperature signal still present in the output from the velocity wires and vice versa for the temperature wire. The need for this can be seen from the error analysis presented in the Appendix.

A P.A.R. Model 100 cross-correlator was used to measure the time delayed cross-correlations.

EXPERIMENTAL RESULTS

Radial velocity and temperature distributions

To check that a generally accepted fully developed velocity field had been obtained, the radial velocity distribution was measured under isothermal conditions at several Reynolds numbers using a pitot tube. Excellent agreement was obtained with the universal velocity profile in the log layer region but in the core region of the flow the usual deviation from the latter was found. The present results also agree with Laufer's [17] who considered only fully developed pipe flow.

Radial temperature profiles were compared with those of Johnk and Hanratty [18]. No significant difference between the present temperature profiles and those of the quoted authors was found other than that which must be expected because of buoyancy effects which were

noticeable in the present case as the tube was horizontal. The effect of shortening the heated length was also investigated to ensure that fully developed conditions had been attained but no difference between the long and short sections was detected. A radial temperature profile is shown in Fig. 1. Part of the traverse is reflected about the tube centre line in order to emphasise the buoyancy effect.

The friction factor was obtained from axial wall pressure drop measurements in isothermal flow. This agreed with the Blasius relationship, equation (4),

$$f = 0.079 (Re)^{-0.25}. \quad (4)$$

Instead of using the usual definition of U_τ based on wall shear stress and density evaluated at the wall temperature when dealing with non-isothermal streams, the results presented here were obtained by finding Re evaluated at the bulk temperature at the traversing station, calculating f from equation (4) and U_τ from equation (5)

$$U_\tau = \bar{U} \sqrt{\frac{f}{2}}. \quad (5)$$

This simplification is justified as the temperature differences in the stream were not very large.

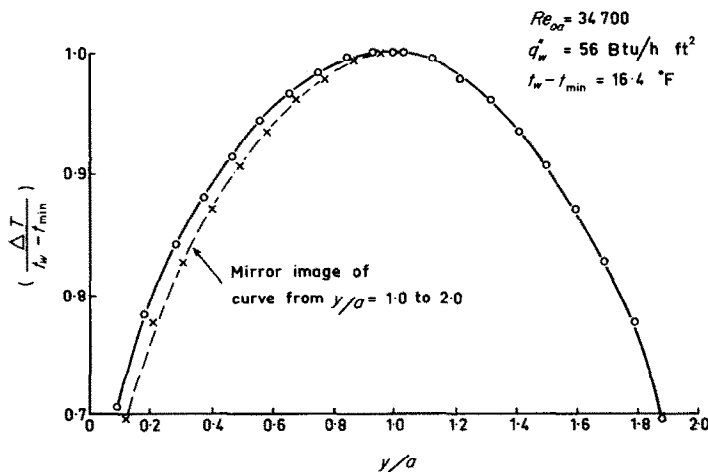


FIG. 1. Typical radial temperature profile.

Fluctuating quantities

When using constant current hot wire anemometers the directly measured quantities are $(\sqrt{u^2})/U$ and $\sqrt{\delta^2}$. In order to normalise the latter on a parameter equivalent to U the temperature difference (ΔT) between the wall and the stream at the particular y can be used. ΔT was measured with thermocouples. The two normalised intensity distributions as a function of y/a are shown in Fig. 2.

The same quantities normalised on U_r and T_r are shown in Fig. 3 where the range of $(\sqrt{u^2})/U_r$ measured by Laufer [17] and by Sandborn [19] is shown for comparison. The slight drop-off near the wall of the present results is due to a wire length effect.

The remaining quantity of interest is the axial eddy heat transfer represented by the cross product $\overline{u\delta}$. This is shown in normalised form in Fig. 4.

At the tube centre line, $\overline{u\delta}$ does not vanish even though in this region isotropy is generally thought to be approached. A finite $\overline{u\delta}$ must, however, exist because of the linear axial stream temperature gradient. $\overline{u\delta}/U_r T_r$ is seen to increase steadily as the tube wall is approached. A similar trend was observed for $R_{u\delta}$ (Fig. 9) which shows that the fluctuating temperature field is highly correlated with the fluctuating longitudinal velocity field.

Spectral results

Figures 5a–5d show the spectra of u , δ and $u\delta$ presented in the special form discussed previously. An important technicality is that because of the very low frequency cut-off used in the signal processing system, total signal energies were measured with negligible loss of low frequency components. Spectral analyses were, however, limited at low frequencies by the analysers, the available speed-up factor on the tape recorder and most important of all, the very long signal recordings required if still lower frequency spectra are to be obtained with reasonable accuracy. It should be noted that for the low frequency (or wavenumber) data presented, signal recordings of 20 min duration were required. For $y/a = 1.0$ and 0.842, the spectra were almost identical and only the latter is shown.

Since the total intensities are almost identical (refer Fig. 2), it is seen that at all radial positions tested, the temperature fluctuations contain more high frequency energy than the u fluctuations. The benefit of plotting spectra in the manner used here is also obvious. In the core region of the flow, the spectra are single peaked. The range of wavenumbers containing the energy of the velocity and temperature fluctuations is clearly visible and appears to be no more than one to one-and-a-half decades.

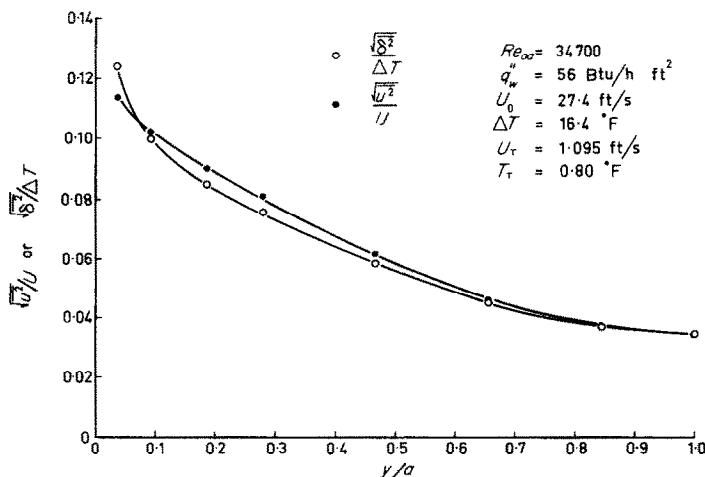


FIG. 2. Intensities of u and δ relative to U and δT .

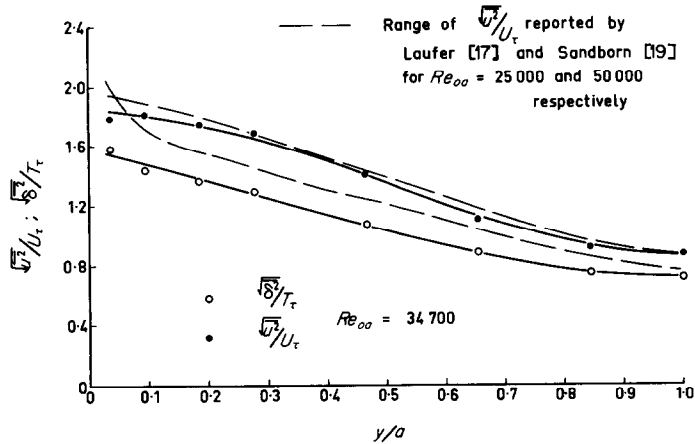
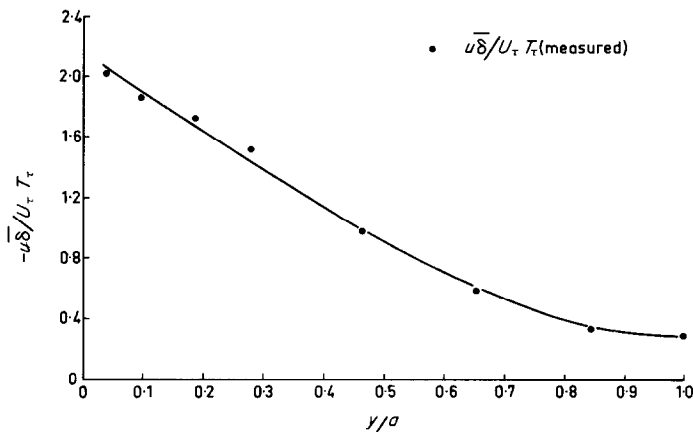
FIG. 3. Intensities of u and δ relative to U_τ and T_τ .

FIG. 4. Axial eddy heat transfer.

Approaching the wall, near $y/a \approx 0.655$, a distinct second peak develops. This is approximately one decade below that of the original peak. As y/a decreases this low wavenumber peak is seen to increase in significance whereas the higher wavenumber peak decreases until at $y/a \approx 0.0935$ or $y^+ \approx 130$, this low wavenumber peak is seen to decrease again accompanied by an increase in the original high wavenumber peak.

With the aid of the results of Morrison [16] and Johnson [3], it is possible to extend the present

results which do not give any detail of the rather vital wall region. From Johnson it can be deduced that close to the wall $R_{\mu\delta} \rightarrow 1.0$ as $y/a \rightarrow 0$. Therefore, the temperature fluctuations must follow the longitudinal velocity fluctuations still more closely. Thus the spectra of δ must approach those of u even closer than those at the y/a presented here. Also, from Morrison's results it is known that as y/a decreases below the values reached here, the low wavenumber peak does in fact disappear as indicated by the trend of the present results and

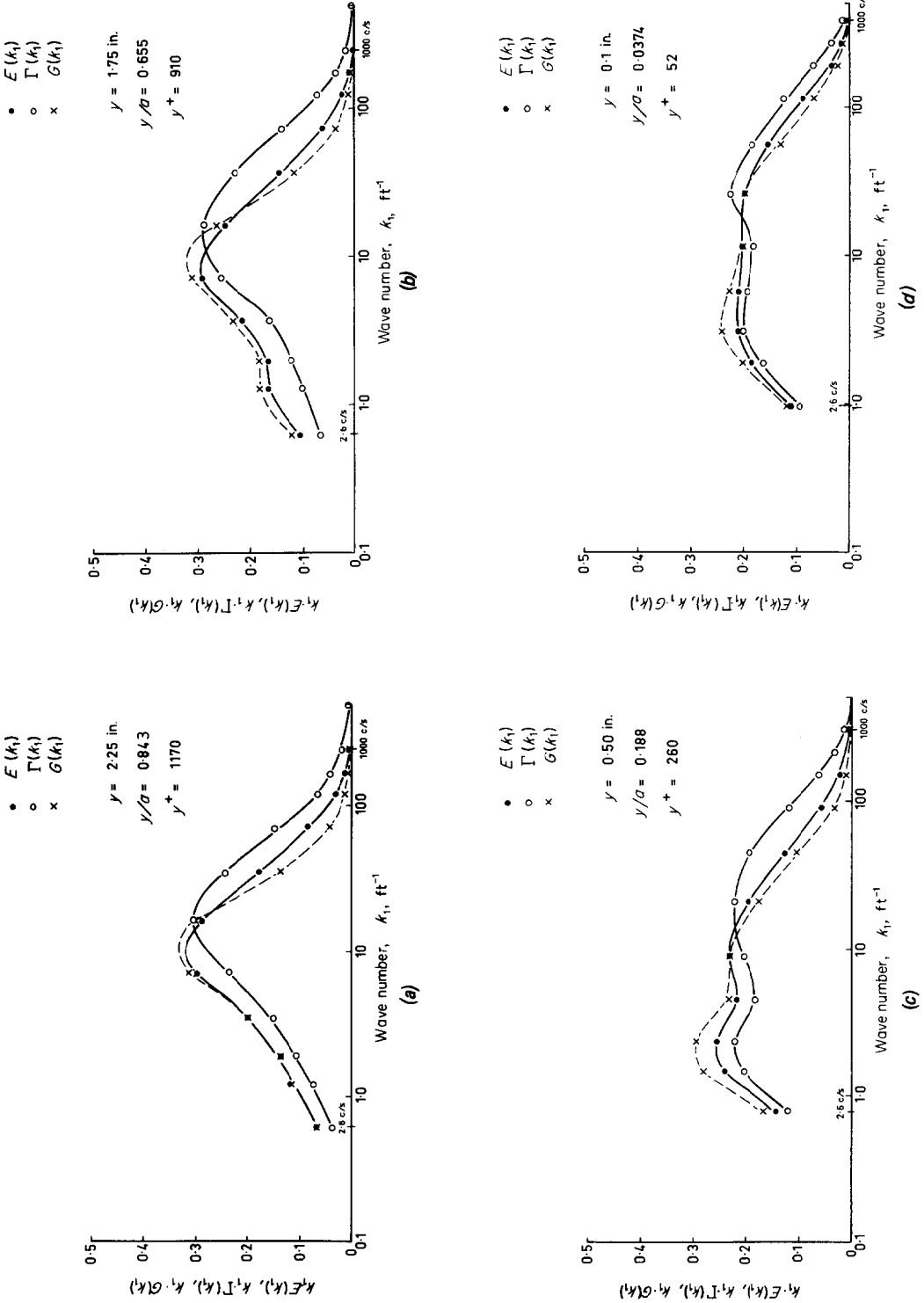
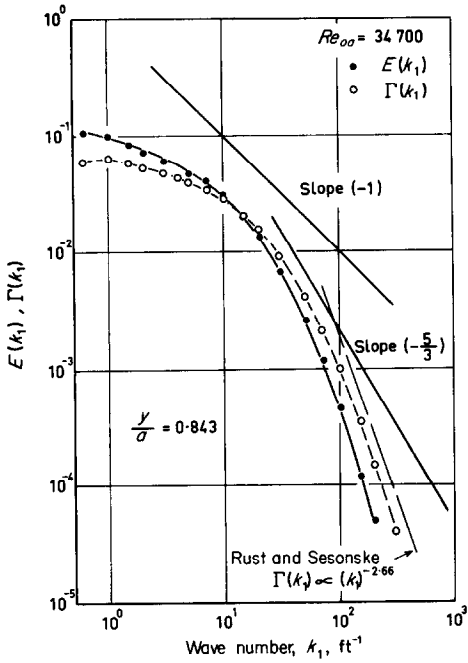
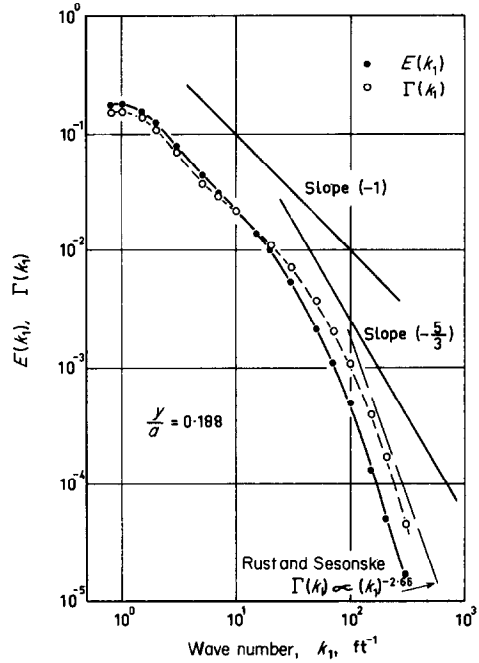


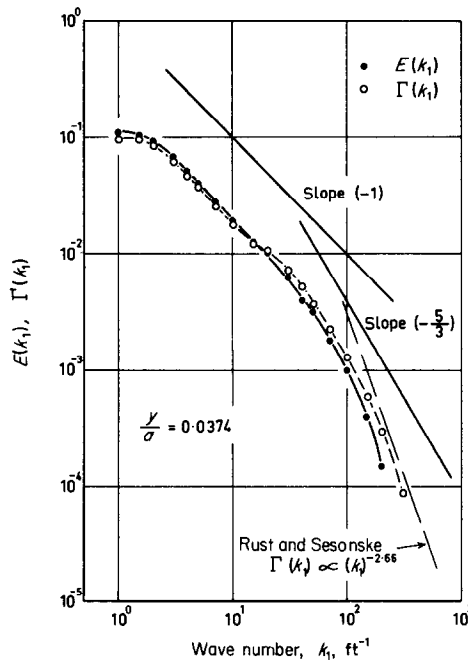
FIG. 5. (a)-(d) Linear-log plots of $E(k_1)$, $\Gamma(k_1)$ and $G(k_1)$ for $Re_{0a} = 34700$.



(a)



(b)



(c)

FIG. 6. (a)-(c) Log-log plots of $E(k_1)$ and $\Gamma(k_1)$ for $Re_{0a} = 34700$.

the high wavenumber peak reappears at almost the same value of k_1 as that found at the larger values of y/a . Thus single peaked spectra are again obtained. (For these results, Morrison measured convection velocities and hence found the true wavenumber.)

Combination of the results shows that the temperature spectrum can be expected to do the same and return to a single peaked spectrum at lower y/a with this peak occurring at almost the same wavenumber as the core region peak of the longitudinal velocity fluctuation spectrum.

The cross-spectrum of $u\delta$ is seen to follow the shape of the spectra of u and δ , the natural result of a high correlation between u and δ . At low wavenumbers and $y/a < 0.655$, the peaks of the three spectra are seen to occur at the same k_1 . The range of wavenumbers is almost the same at all y/a .

Spectra of u and δ have also been plotted in the conventional log-log form. These are shown in Figs. 6a-c for three values of y/a . Lines indicating the usual -1 and $-5/3$ power laws are included for comparison. In the core region of the flow (Fig. 6a) a continuously curved spectrum is indicated which does not have any of the traditional power law regions. For the other two positions, a definite region with slope -1 is seen to exist. This corresponds to the span of wavenumbers covered by the two peaks in

Figs. 5b-d and identifies the energy containing wavenumbers. Tchen [20] has identified this region as one where the vorticity of the main motion is so large that the dominant feature of the flow is an interaction of this vorticity with the turbulent motion rather than one of viscous dissipation and eddy transfer. Such a phenomenon could, perhaps, explain the presence of the lower wavenumber peak.

None of the spectra show the predicted $-5/3$ characteristic at the higher wavenumbers. In fact, the present results and those of Rust and Sesonske [14] which are also shown in Figs. 6a-c indicate a $-8/3$ slope. However, since neither the present nor the quoted authors' results have been corrected for effect of probe size, it is difficult to draw any definite conclusions from this. The remarkable similarity over the lower wavenumber ranges of the u and δ spectra close to the wall is again noticed. At the higher wavenumbers the theoretical prediction that u and δ spectra should have similar slopes is also confirmed although the present results do not really extend very far into the universal subrange.

The results of Tanimoto and Hanratty [13] are shown in Fig. 7. As local velocity data were not available, the authors' original non-dimensionalisation was retained. Thus only the shapes of the spectra should be comparable with the present results. Comparison with Fig.

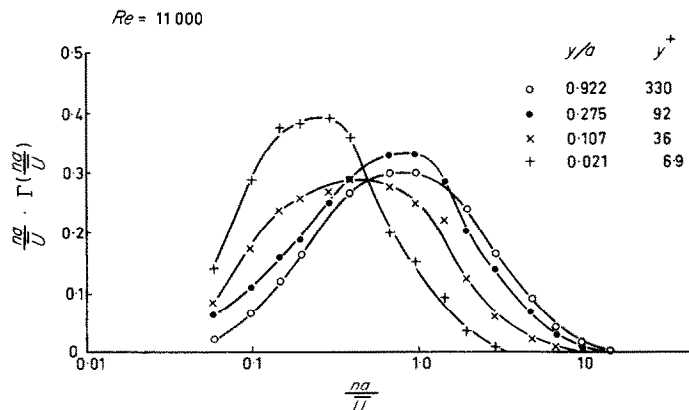


FIG. 7. Temperature fluctuation spectra reported by Tanimoto and Hanratty.

5a shows that the two spectra at or near $y/a = 1.0$ are almost identical. An obvious difference between the present results and those of Fig. 7 is, however, that no double peaks were found by Tanimoto and Hanratty. The explanation for this is simple. Morrison found that at very low Reynolds numbers ($Re \approx 22000$ or $Re_{0a} \approx 17000$ and below) the u spectrum does not show a double peaked shape at least for the y/a tested by him, whereas for higher Reynolds numbers the double peaks are a definite characteristic as confirmed by the present results. Thus, assuming that u and δ spectra show the same similarity at low Reynolds numbers, it is clear that no double peaks should appear in Fig. 7. The present results are, therefore, an addition to existing data and outline a very distinctive feature of the flow regime corresponding to the flow region generally identified as the logarithmic layer.

From Figs. 5a-d and the definition of k_1 it is seen that the spectral peak in the core region of the flow is associated with $\lambda_1 = 4.5-7.5$ in., which is of the order of the tube diameter. The log layer peak, that is the second peak which occurred at lower wavenumbers, is associated with $\lambda_1 = 37$ in., which is almost seven times the tube diameter. The data show, therefore that u and δ have a considerable amount of energy at wavelengths equal to and much greater than the tube diameter.

Cross-spectral correlation coefficients

From the measurements, cross-spectral (or narrow band) correlation coefficients were also determined. These are shown as a function of wavenumber in Fig. 8 and as a function of y/a in Fig. 9 which also shows the total correlation coefficient for comparison. In Fig. 8 a near perfect correlation is indicated at very low wavenumbers. At high wavenumbers zero correlation is approached, thus indicating a trend towards isotropy. The higher correlations at high wavenumbers near the wall are also clearly seen and are further emphasised by Fig. 9 in which the correlations with decreasing y/a have been shown dotted on the assumption that $R_{u\delta} = 1.0$ at $y/a = 0$. These results further emphasise the close relationship between u and δ and with the aid of Figs. 6a-c it is seen that the highest correlation is generally associated with the most energetic flow components.

Although one-dimensional spectral data give a very incomplete description of the flow structure, some conclusions concerning the flow can be offered with the aid of the hydrogen visualisation data of Rundstadler *et al.* [21]. The latter found that near the wall the flow has a streaky nature which appears to have a well defined transverse wavelength. These streaks are highly inclined so that their direction is almost in the flow direction. Periodically, these streaks break away from the wall and disperse into the main

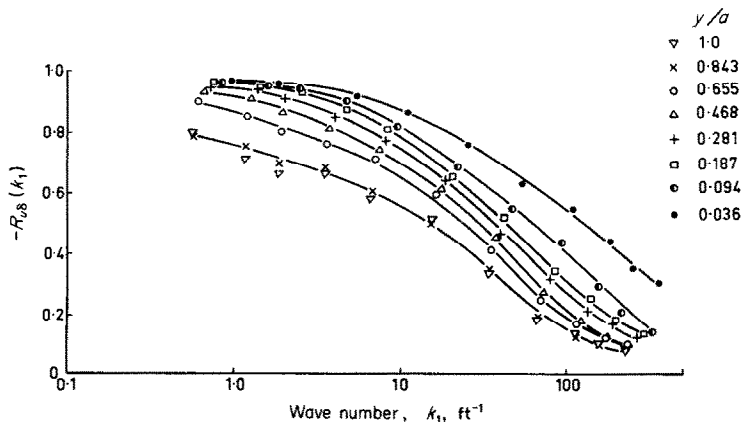


FIG. 8. Spectral correlation coefficient as a function of k_1 for $Re_{0a} = 34700$.

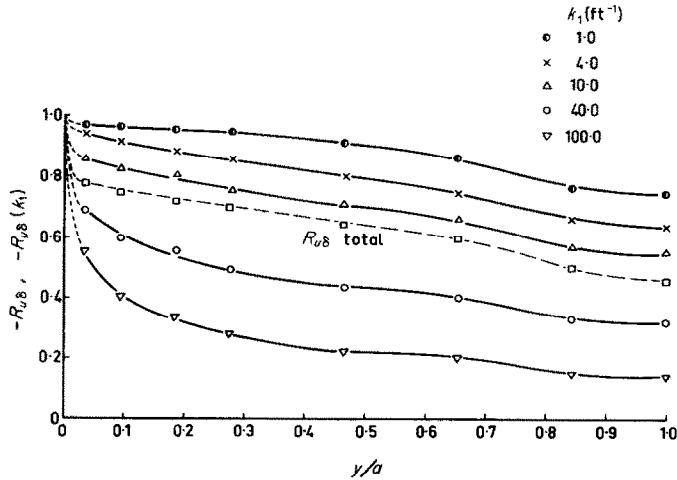


FIG. 9. Spectral correlation coefficient as a function of y/a .

flow. At the wall, the streaks can be expected to show near perfect correlation between u and δ . As these fluid streaks (or lumps) which break away retain their identity (in a Lagrangian sense) for a long time, and if these are elongated even further by interaction with the main flow, they can, in fact, become responsible for the low wavenumber contributions which have high values of $R_{u\delta}(k_1)$ as well as the double peaked spectrum in the logarithmic layer.

Alternatively, it may be argued quite independently of the above visualisation data, that large scale phenomena which extend throughout the whole flow are associated with the low wave-

numbers and that because these large and highly energetic components (refer Figs. 6a-c) retain their identity longer, better correlations can be expected as is, in fact, shown by the experimental data.

$R_{u\delta}$ was also measured in the above flow but with a heated length of only 27 tube diameters. No significant difference was noted thus indicating that either $R_{u\delta}$ had reached its fully developed value or was approaching it asymptotically. It is reasonable to assume, therefore, that the present results were obtained in a fully developed flow.

Large values of $R_{u\delta}$ even at the centre line of

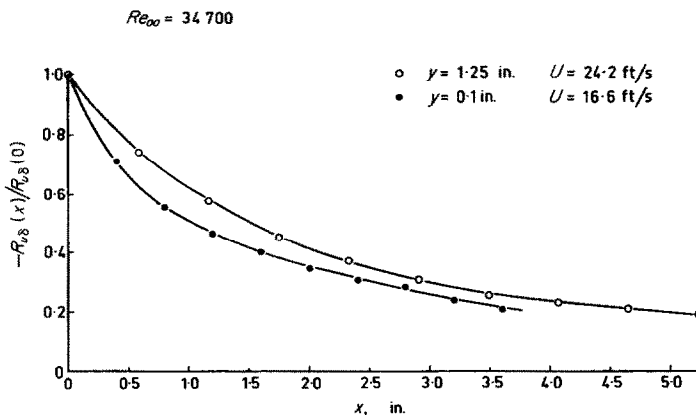


FIG. 10. Streamwise correlation between u and δ for $Re_{0m} = 34700$.

the flow must, of course, be expected when using constant heat flux heating since a linear axial temperature gradient exists at all points from the wall. This does not necessarily hold for constant wall temperature heating for which the axial temperature gradient is non-linear.

Time delayed cross-correlations

Intuitively, it is felt that there should be no simple time constant effects which influence the relationship between u and δ . One method of testing this is to show that the quad-spectrum of u and δ (the cross-spectrum measured above is the co-spectrum) is zero at all k_1 . A simpler method of showing this is to find the time delayed cross-correlation between u and δ by delaying and advancing one signal relative to the other. If the resultant cross-correlation is symmetrical about zero time shift, the quad-spectrum does indeed vanish. Such a test was carried out at two values of y/a . It was found that a completely symmetrical correlation exists thus confirming the above theory.

If it is assumed that the whole turbulent field convects at the local velocity, which is Taylor's hypothesis, then the time delayed correlation coefficient between u and δ can be converted to a spatial one, $R_{u\delta}(x)$. This is shown in Fig. 10 and indicates that u and δ are correlated even for separations of the order of magnitude of the tube diameter. This, of course, follows from the high correlation between u and δ and the large stream-wise correlation of u .

Measurement at other Reynolds numbers and possible effects due to buoyancy

In order to test the observed results for Reynolds number dependency, similar data were collected at a Reynolds number of 155000. Identical trends to those presented were obtained but the spectra were slightly distorted. This was thought to be due to a flow interference effect due to the complex wire and wire support array which attenuated the high frequency contributions. The double peaked spectral trends were, however, confirmed and single peaked

spectra were again obtained for the range $y/a \approx 1.0-0.655$. This phenomenon appears therefore, to follow a y/a scaling and corresponds closely to the deviation in the core region of the universal velocity profile from the logarithmic relationship.

The disappearance of the lower wavenumber peak was not observed but with the aid of Morrison's data and the high $R_{u\delta}$ observed in the present work, it was deduced that at $y^+ \approx 50-60$ spectra again should become single peaked with decreasing y/a . In this region of the flow y^+ , not y/a , was found to be the scaling parameter. The wavenumber ranges in all cases were very nearly the same as those at the lower Reynolds number.

From the mean temperature profile given in Fig. 1 it is obvious that some buoyancy effects existed in the flow. In order to check whether the buoyancy induced secondary flow patterns were significant, $E(k_1)$ as reported for the non-isothermal tests of Figs. 5a-c was compared with the $E(k_1)$ measured in the unheated air stream using the same equipment and measurement techniques. This was considered to be the most sensitive test of the buoyancy effect. No significant differences were noted in the spectra except for a decrease of less than 10 per cent in the low frequency energy for the isothermal flow. Since buoyancy would most probably introduce a low frequency component, the trend in the measurements was consistent with expectations but it was considered insignificant for present purposes.

CONCLUSIONS

The measurements showed that the intensities of the longitudinal velocity and temperature fluctuations are nearly identical when normalized on the local mean velocity and the mean temperature difference respectively. A large axial component of eddy heat transfer was found to exist even at the centre line of the tube. This showed a considerable increase towards the wall of the flow. The correlation coefficient between longitudinal velocity and temperature

fluctuations varied from 0.48 at the centre line of the tube to 0.78 at $y/a = 0.037$. For positions still closer to the wall a trend of this coefficient towards unity is indicated.

Spectral results presented on the linear-log plot showed the following features. In the core region of the flow single peaked spectra exist centred about $k_1 = 10 \text{ ft}^{-1}$ for the velocity spectrum and 20 ft^{-1} for the temperature spectrum. As the wall was approached, for $y/a = 0.655$ and less, a second but lower wavenumber peak developed. This flow region corresponds to the familiar logarithmic layer. Temperature and velocity spectra were found to be very similar but temperature spectra had more energy at large k_1 than velocity spectra. The core region peak was shown to represent wavelengths of the order of the tube diameter but the second peak was associated with much larger wavelengths thus indicating the importance of the large scale structure near the wall.

Spectra plotted on the usual log-log plot verified the existence of a region with a slope of -1 in the logarithmic layer of the flow but not in the core region. This span of k_1 corresponds to the range of wavenumbers containing a significant proportion of the fluctuating energy. The most energetic flow components always existed at the lower end of this range of k_1 .

Cross-spectra behaved similarly to those of the individual velocity and temperature spectra, tending to be above these at low k_1 and below at the large values of k_1 . Values of the cross-correlation coefficient extracted from the results indicated almost perfect correlation between u and δ at low k_1 but a gradual decrease to almost zero at large k_1 . Thus almost perfect analogy exists between heat and momentum transfer at low k_1 , or the large and energetic components of the flow. This agrees with the known asymptotic limit of perfect analogy for laminar flows. The trend towards zero correlation at large k_1 implies that the majority of the axial eddy heat transfer is associated with the lower wavenumber components which was verified by the cross-spectral results.

Application of Taylor's hypothesis to time delayed correlations provided further spatial information. This showed that the longitudinal velocity and temperature fluctuations are well correlated over distances equal to one quarter of the tube diameter and moderately correlated for separations equal to the tube diameter.

The results, therefore, indicate that in a fully developed flow, heat and momentum are very closely related at low and medium wavenumbers but not at the higher ones. The latter observation is characteristic of the beginning of the universal subrange in which the behaviour of the flow becomes independent of its method of formation. Measurements involving the radial velocity fluctuations are, however, still required in order to supplement the above findings before a realistic mechanism for fully developed turbulent heat transfer can be proposed.

ACKNOWLEDGEMENT

The authors are most grateful to the Australian Institute of Nuclear Science and Engineering for their substantial support of the project of which the present results are an essential part.

REFERENCES

1. E. R. G ECKERT and R. M. DRAKE, *Heat and Mass Transfer*, pp. 202-203. McGraw-Hill, New York (1959).
2. J. KESTIN and P. D. RICHARDSON, Heat transfer across turbulent, incompressible boundary layers, *Int. J. Heat Mass Transfer* **6**, 147-189 (1963).
3. D. S. JOHNSON, Velocity and temperature fluctuation measurements in a turbulent boundary layer downstream of a stepwise discontinuity in wall temperature *J. Appl. Mech.* **81**, 325-336 (1959).
4. S. CORRISIN, Further generalization of Onsager's cascade model for turbulent spectra, *Physics Fluids* **7**, 1156-1159 (1964).
5. A. M. OBUCKHOFF, *Izv. Akad. Nauk, U.S.S.R., Geogr. i Geofiz.* **13**, 58 (1949).
6. G. K. BATCHELOR, Small scale variations of convected quantities like temperature in turbulent fluids—Part 1 *J. Fluid Mech.* **5**, 113-133 (1959).
7. G. K. BATCHELOR, I. D. HOWELLS and A. A. TOWNSEND, Small scale variations of convected quantities like temperature in turbulent fluids—Part 2, *J. Fluid Mech.* **5**, 134-139 (1959).
8. G. H. GIBSON and W. H. SCHWARZ, The universal equilibrium spectra of turbulent velocity and scalar fields, *J. Fluid Mech.* **16**, 365-385 (1963).
9. J. O. HINZE, *Turbulence*, pp. 268-269. McGraw-Hill, New York (1959).

10. *Ibid.* pp. 263–268.
11. S. CORRISIN *et al.*, Turbulence and temperature fluctuations behind a heated grid, N.A.C.A. Tech. Note 4288 (1958).
12. H. L. GRANT, B. A. HUGHES, W. M. VOGEL and A. MOILLIET, The spectrum of temperature fluctuations in turbulent flow, *J. Fluid Mech.* **34**, 423–442 (1968).
13. S. TANIMOTO and T. J. HANRATTY, Fluid temperature fluctuations accompanying turbulent heat transfer in a pipe, *Chem. Engng Sci.* **18**, 307–311 (1963).
14. J. H. RUST and A. SESONSKE, Turbulent temperature fluctuations in mercury and ethylene glycol in pipe flow, *Int. J. Heat Mass Transfer* **9**, 215–227 (1966).
15. S. CORRISIN and M. S. UBEROI, Spectra and diffusion in a round turbulent jet, N.A.C.A. Report 1040 (1949).
16. W. R. B. MORRISON, Two dimensional frequency-wavenumber spectra and narrow band shear stress correlations in turbulent pipe flow, Ph.D. Thesis, University of Queensland, Australia (1969).
17. J. LAUFER, The structure of turbulence in fully developed pipe flow, N.A.C.A. Report 1174 (1954).
18. R. E. JOHNK and T. J. HANRATTY, Temperature profiles for turbulent flow of air in a pipe, *Chem. Engng Sci.* **17**, 374 (1962).
19. V. A. SANDBORN, Experimental evaluation of momentum terms in turbulent pipe flow, N.A.C.A. Tech. Note TN3266 (1955).
20. TSCHEN—refer HINZE Ref. [10].
21. T. W. RUNDSTADLER, S. J. KLINE and W. C. REYNOLDS, An experimental investigation of the flow structure of the turbulent boundary layer, Stanford University, Mech. Engng Dept., Thermosciences Div., Report MD8 (1963).
22. K. BREMHORST, On the similarity of heat and momentum transfer in turbulent pipe flow, Thesis (Ph.D.), University of Queensland, Australia (1969).

APPENDIX

Error Analysis

The purpose of this section is not to discuss general errors encountered in hot wire anemometer measurements, but to show that because of the dual response characteristic of a hot wire anemometer in non-isothermal flow, large errors in the measurement of \bar{u}_δ and $R_{u\delta}$ are obtained unless great care is taken to remove unwanted signal components.

For the present experiments, the voltages from the two inclined wires were summed and differenced simultaneously on the analogue computer to give signals which were nominally proportional to the longitudinal and radial velocity fluctuations. Prior to this operation the amplitudes of the inclined wire signals were, of course, adjusted for the slightly different directional sensitivities of the two wires as it was found to be a near impossible task to manufacture and position a perfectly symmetrical X-meter in the tube. The signal which is mainly proportional to u is

$$e_{ux} = -K_{Ax}K_{ux}u + K_{Ax}K_{\delta x}\delta \quad (\text{A.1})$$

where K_{Ax} is the amplifier gain and K_{ux} and $K_{\delta x}$ are the

respective wire sensitivities to u and δ . Similarly, the output of the temperature wire is

$$e_{\delta 1} = -K_{A1}K_{u1}u + K_{A1}K_{\delta 1}\delta. \quad (\text{A.2})$$

Since the velocity wires were operated at a very high temperature and the temperature wire at a very low temperature, it may be argued that

$$K_{ux} \gg K_{\delta x}$$

and

$$K_{u1} \ll K_{\delta 1}$$

thus reducing equations (A.1) and (A.2) to

$$e'_{ux} = -K_{Ax}K_{ux}u \quad (\text{A.3})$$

and

$$e'_{\delta 1} = +K_{A1}K_{\delta 1}\delta \quad (\text{A.4})$$

where the prime denotes the approximate response. If e'_{ux} and $e'_{\delta 1}$ are now spectrally analysed, spectra of u and δ are available. If two identical analysers are available, these can then be aligned and e'_{ux} passed through one and $e'_{\delta 1}$ through the other. Multiplication of the two signals followed by integration or averaging gives $\overline{u(k_1)\delta(k_1)}$ as required. Unfortunately, this would lead to considerable errors especially in $\overline{u(k_1)\delta(k_1)}$ and $R_{u\delta}(k_1)$ because even at high wire temperatures, the velocity wires still contain a significant temperature component. To visualize this more readily, equation (A.1) and (A.2) can be written as

$$e = -K_A K_u U \frac{u}{U} + K_A K_\delta \Delta T \frac{\delta}{\Delta T} \quad (\text{A.5})$$

where U is the local mean velocity and ΔT is the difference between the wall temperature and the local fluid temperature. The relative sensitivity of a wire to either u or δ is then defined by the ratio of $K_u U / K_\delta \Delta T$.

The relevant percentage errors in $(\sqrt{u^2})/U$, $(\sqrt{\delta^2})/\Delta T$ and $\overline{u\delta}/U\Delta T$ can be found by simple algebraic manipulation of the above equations and are

$$\begin{aligned} \epsilon_u &= \text{Error in } \frac{\sqrt{u^2}}{U} \\ &= \frac{1}{2} \left(\frac{K_{\delta x} \Delta T}{K_{ux} U} \right)^2 \frac{\overline{\delta^2}/(\Delta T)^2}{\overline{u^2}/U^2} \\ &\quad - \left(\frac{K_{\delta x} \Delta T}{K_{ux} U} \right) R_{u\delta} \frac{(\sqrt{\delta^2})/\Delta T}{(\sqrt{u^2})/U} \end{aligned} \quad (\text{A.6})$$

$$\begin{aligned} \epsilon_\delta &= \text{Error in } \frac{(\sqrt{\delta^2})}{\Delta T} \\ &= \frac{1}{2} \left(\frac{K_{u1} U}{K_{\delta 1} \Delta T} \right)^2 \frac{\overline{u^2}/U^2}{\overline{\delta^2}/(\Delta T)^2} \\ &\quad - \left(\frac{K_{u1} U}{K_{\delta 1} \Delta T} \right) R_{u\delta} \frac{(\sqrt{u^2})/U}{\sqrt{\delta^2}/\Delta T} \end{aligned} \quad (\text{A.7})$$

$$\begin{aligned} \epsilon_{u\delta} &= \text{Error in } \frac{\overline{u\delta}}{U\Delta T} \\ &= - \left[\left(\frac{K_{u1}U}{K_{\delta1}\Delta T} \right) \frac{(\sqrt{u^2})/U}{(\sqrt{\delta^2})/\Delta T} + \frac{K_{\delta x}\Delta T}{K_{ux}U} \frac{(\sqrt{\delta^2})/\Delta T}{(\sqrt{u^2})/U} \right] \frac{1}{R_{u\delta}} \\ &\quad + \left(\frac{K_{u1}U}{K_{\delta1}\Delta T} \right) \left(\frac{K_{\delta x}\Delta T}{K_{ux}U} \right). \quad (\text{A.8}) \end{aligned}$$

For the present experiments the inclined wires were operated at a mean wire temperature of 530°F and the temperature wire at 3–4°F above the local stream temperature. Thus,

$$\frac{K_{ux}U}{K_{\delta x}\Delta T} \approx 10$$

and

$$\frac{K_{\delta1}\Delta T}{K_{u1}U} \approx 20.$$

For fully developed tube flow $[(\sqrt{u^2})/U] \approx [(\sqrt{\delta^2})/\Delta T]$ and $R_{u\delta}$ is negative. If $|R_{u\delta}|$ denotes the absolute value of $R_{u\delta}$, equations (A.6)–(A.8) reduce to,

$$\epsilon_u \approx +10|R_{u\delta}| \text{ per cent} \quad (\text{A.9})$$

$$\epsilon_\delta \approx +5|R_{u\delta}| \text{ per cent} \quad (\text{A.10})$$

and

$$\epsilon_{u\delta} \approx + \frac{15}{|R_{u\delta}|} \text{ per cent.} \quad (\text{A.11})$$

Since $|R_{u\delta}|$ is typically 0.5–1.0, it is seen that $\epsilon_u \approx 5$ –10 per cent, $\epsilon_\delta \approx 2.5$ –5 per cent and $\epsilon_{u\delta} \approx 30$ –15 per cent. The error in $R_{u\delta}$ would be 22.5–0.0 per cent. These are all considerable errors. The need for further signal corrections is obvious. Note, however, the benefit obtained by using the present measurement technique, namely that the correction can be very inaccurate. For example, if the correction is only 50 per cent of that needed, the errors are approximately halved which is a worthwhile improvement. Such a correction was therefore introduced into the analogue computer program and effectively involved the simultaneous solution of equations (A.1) and (A.2) which is, of course, very simple to perform. Full details of this are available in [22].

The above error analysis applies to total as well as spectral results but for the latter it must be realised that $(\sqrt{u^2}(k_1)/U)$ is not approximately equal to $\sqrt{\lambda^2(k_1)}/\Delta T$ at all k_1 . Thus the above errors can be even larger, depending on the relative magnitudes of the two spectra at a given k_1 . This further emphasizes the need for the extra correction.

MESURES DES SPECTRES DES FLUCTUATIONS DE TEMPÉRATURE ET DE VITESSE LONGITUDINALE DANS DES ÉCOULEMENTS EN CONDUITE ENTIÈREMENT ÉTABLIS

Résumé—On sait que pour des écoulements entièrement établis, la similitude entre le transport de chaleur et celui de quantité de mouvement peut être étudiée à l'aide des fluctuations de température et de vitesse longitudinale en un point. Des résultats de mesures des spectres et des spectres croisés sont présentés qui montrent qu'il existe une relation étroite entre les champs de vitesse et de température aux faibles nombres d'ondes mais non aux nombres d'onde élevés. On a trouvé un flux d'énergie considérable associé à des longueurs d'onde beaucoup plus grandes que le diamètre du tube et de nouvelles informations sur les formes des spectres ont été révélées. L'étendue en aval de la corrélation entre les deux champs est décrite à partir de l'hypothèse de Taylor et des corrélations croisées avec décalage temporel.

MESSUNGEN DES SPEKTRUMS VON TEMPERATUR- UND LÄNGSGESCHWINDIGKEITSÄNDERUNGEN BEI VOLL AUSGEBILDETER ROHRSTRÖMUNG

Zusammenfassung—Es ist bekannt, dass für voll ausgebildete Strömungen die Ähnlichkeit zwischen Wärme- und Impulsübertragung an Hand von Temperaturänderungen und Änderungen der Längsgeschwindigkeit an ein und demselben Punkt studiert werden kann.

Ergebnisse von Messungen des Turbulenzspektrums und von Kreuz- und Korrelationsmessungen zeigen, dass eine strenge Beziehung zwischen Geschwindigkeits- und Temperaturfeld bei niedrigen, nicht jedoch bei hohen Wellenzahlen besteht, wobei unter Wellenzahl eine auf die Konvektionsgeschwindigkeit bezogene Frequenz verstanden wird.

Bei Wellenlängen, die viel grösser sind als der Rohrdurchmesser, wurde eine beachtenswerte Strömungsenergie beobachtet. Neue Informationen über die Formen der Spektren werden dargelegt.

Ausgehend von der Taylor-Hypothese und von zeitverzögerten Kreuz-Korrelationen wird der strömungsmässige Umfang der Korrelation zwischen den beiden Feldern beschrieben.

СПЕКТРАЛЬНЫЕ ИЗМЕРЕНИЯ ПУЛЬСАЦИЙ ТЕМПЕРАТУРЫ
И ПРОДОЛЬНОЙ СКОРОСТИ В ПОЛНОСТЬЮ РАЗВИТОМ
ПОТОКЕ В ТРУБЕ

Аннотация—Известно, что подобие между переносом тепла и импульса для полностью развитых потоков можно исследовать с помощью локальных пульсаций температуры и продольной скорости. Представлены результаты спектральных и поперечно-спектральных измерений, которые показывают, что при низких волновых числах существует тесная зависимость между полями скоростей и температур, отсутствующая при высоких волновых числах. Установлено, что с длиной волны, гораздо большей диаметра трубы, связан значительный поток энергии. Получены новые сведения о формах спектра. Используя гипотезу Тейлора и задержку по времени измеряемых корреляций, описана связь между двумя полями вдоль линии тока.